

A CUDA-Based Real Parameter Optimization Benchmark

Ke Ding and Ying Tan

School of Electronics Engineering and Computer Science, Peking University

Abstract. Benchmarking is key for developing and comparing optimization algorithms. In this paper, a CUDA-based real parameter optimization benchmark (cuROB) is introduced. Test functions of diverse properties are included within cuROB and implemented efficiently with CUDA. Speedup of one order of magnitude can be achieved in comparison with CPU-based benchmark of CEC'14.

Key words: Optimization Methods, Optimization Benchmark, GPU, CUDA.

1 Introduction

Proposed algorithms are usually tested on benchmark for comparing both performance and efficiency. However, as it can be a very tedious task to select and implement test functions rigorously. Thanks to GPUs' massive parallelism, a GPU-based optimization function suit will be beneficial to test and compare optimization algorithms.

Based on the well known CPU-based benchmarks presented in [1–3], we proposed a CUDA-based real parameter optimization test suit, called cuROB, targeting on GPUs. We think cuROB can be helpful for assessing GPU-based optimization algorithms, and hopefully, conventional CPU-based algorithms can benefit from cuROB's fast execution.

Considering the fact that research on the single objective optimization algorithms is the basis of the research on the more complex optimization algorithms such as constrained optimization algorithms, multi-objective optimizations algorithms and so forth, in this first release of cuROB a suit of single objective real-parameter optimization function are defined and implemented.

The test functions are selected according to the following criteria: 1) the functions should be scalable in dimension so that algorithms can be tested under various complexity; 2) the expressions of the functions should be with good parallelism, thus efficient implementation is possible on GPUs; 3) the functions should be comprehensible such that algorithm behaviours can be analysed in the topological context; 4) last but most important, the test suit should cover functions of various properties in order to get a systematic evaluation of the optimization algorithms.

The source code and a sample can be download from code.google.com/p/curob/.

1.1 Symbol Conventions and Definitions

Symbols and definitions used in the report are described in the following. By default, all vectors refer to column vectors, and are depicted by lowercase letter and typeset in bold.

- $\lceil \cdot \rceil$ indicates the nearest integer value
- $\lfloor \cdot \rfloor$ indicates the largest integer less than or equal to
- \mathbf{x}_i denotes i -th element of vector \mathbf{x}
- $f(\cdot)$, $g(\cdot)$ and $G(\cdot)$ multi-variable functions
- f_{opt} optimal (minimal) value of function f
- \mathbf{x}^{opt} optimal solution vector, such that $f(\mathbf{x}^{opt}) = f_{opt}$
- \mathbf{R} normalized orthogonal matrix for rotation
- D dimension
- $\mathbf{1} = (1, \dots, 1)^T$ all one vector

1.2 General Setup

The general setup of the test suit is presented as follows.

- **Dimensions** The test suit is scalable in terms of dimension. Within the hardware limit, any dimension $D \geq 2$ works. However, to construct a real hybrid function, D should be at least 10.
- **Search Space** All functions are defined and can be evaluated over \mathcal{R}^D , while the actual search domain is given as $[-100, 100]^D$.
- f_{opt} All functions, by definition, have a minimal value of 0, a bias (f_{opt}) can be added to each function. The selection can be arbitrary, f_{opt} for each function in the test suit is listed in Tab. 1.
- \mathbf{x}^{opt} The optimum point of each function is located at original. \mathbf{x}^{opt} which is randomly distributed in $[-70, 70]^D$, is selected as the new optimum.
- **Rotation Matrix** To derive non-separable functions from separable ones, the search space is rotated by a normalized orthogonal matrix \mathbf{R} . For a given function in one dimension, a different \mathbf{R} is used. Variables are divided into three (almost) equal-sized subcomponents randomly. The rotation matrix for each subcomponent is generated from standard normally distributed entries by Gram-Schmidt orthonormalization. Then, these matrices consist of the \mathbf{R} actually used.

1.3 CUDA Interface and Implementation

A simple description of the interface and implementation is given in the following. For detail, see the source code and the accompanied readme file.

Interface Only `benchmark.h` need to be included to access the test functions, and the CUDA file `benchmark.cu` need be compiled and linked. Before the compiling start, two macro, `DIM` and `MAX_CONCURRENCY` should be modified accordingly. `DIM` defines the dimension of the test suit to used while `MAX_CONCURRENCY` controls the most function evaluations be invoked concurrently. As memory needed to be pre-allocated, limited by the hardware, don't set `MAX_CONCURRENCY` greater than actually used.

Host interface function `initialize()` accomplish all initialization tasks, so must be called before any test function can be evaluated. Allocated resource is released by host interface function `dispose()`.

Both double precision and single precision are supported through `func_evaluate()` and `func_evaluatef()` respectively. Take note that device pointers should be passed to these two functions. For the convenience of CPU code, C interfaces are provided, with `h_func_evaluate` for double precision and `h_func_evaluatef` for single precision. (In fact, they are just wrappers of the GPU interfaces.)

Efficiency Concerns When configuration of the suit, some should be taken care for the sake of efficiency. It is better to evaluation a batch of vectors than many smaller. Dimension is a fold of 32 (the warp size) can more efficient. For example, dimension of 96 is much more efficient than 100, even though 100 is little greater than 96.

1.4 Test Suite Summary

The test functions fall into four categories: unimodal functions, basic multimodal functions, hybrid functions and composition functions. The summary of the suit is listed in Tab. 1. Detailed information of each function will given in the following sections.

2 Speedup

Under different hardware, various speedups can be achieved. 30 functions are the same as CEC'14 benchmark. We test the cuROB's speedup with these 30 functions under the following settings: Windows 7 SP1 x64 running on Intel i5-2310 CPU with NVIDIA 560 Ti, the CUDA version is 5.5. 50 evaluations were performed concurrently and repeated 1000 runs. The evaluation data were generated randomly from uniform distribution.

The speedups with respect to different dimension are listed by Tab. 2 (single precision) and Tab. 3 (double precision). Notice that the corresponding dimensions of cuROB are 10, 32, 64 and 96 respectively and the numbers are as in Tab. 1

Fig. 1 demonstrates the overall speedup for each dimension. On average, cuROB is never slower than its CPU-base CEC'14 benchmark, and speedup of one order of magnitude can be achieved when dimension is high. Single precision is more efficient than double precision as far as execution time is concerned.

Table 1. Summary of cuROB’s Test Functions

	No.	Functions	ID	Description
Unimodal Functions	0	Rotated Sphere	SPHERE	Optimum easy to track
	1	Rotated Ellipsoid	ELLIPSOID	
	2	Rotated Elliptic	ELLIPTIC	Optimum hard to track
	3	Rotated Discus	DISCUS	
	4	Rotated Bent Cigar	CIGAR	
	5	Rotated Different Powers	POWERS	
	6	Rotated Sharp Valley	SHARPV	
Basic Multi-modal Functions	7	Rotated Step	STEP	With adequate global structure
	8	Rotated Weierstrass	WEIERSTRASS	
	9	Rotated Griewank	GRIEWANK	
	10	Rastrigin	RARSTRIGIN_U	
	11	Rotated Rastrigin	RARSTRIGIN	
	12	Rotated Schaffer’s F7	SCHAFFERSF7	
	13	Rotated Expanded Griewank plus Rosenbrock	GRIE_ROSEN	With weak global structure
	14	Rotated Rosenbrock	ROSENBROCK	
	15	Modified Schwefel	SCHWEFEL_U	
	16	Rotated Modified Schwefel	SCHWEFEL	
	17	Rotated Katsuura	KATSUURA	
	18	Rotated Lunacek bi-Rastrigin	LUNACEK	
	19	Rotated Ackley	ACKLEY	
	20	Rotated HappyCat	HAPPYCAT	
21	Rotated HGBat	HGBAT		
	22	Rotated Expanded Schaffer’s F6	SCHAFFERSF6	
Hybrid Functions	23	Hybrid Function 1	HYBRID1	With different properties for different variables subcomponents
	24	Hybrid Function 2	HYBRID2	
	25	Hybrid Function 3	HYBRID3	
	26	Hybrid Function 4	HYBRID4	
	27	Hybrid Function 5	HYBRID5	
	28	Hybrid Function 6	HYBRID6	
Composition Functions	29	Composition Function 1	COMPOSITION1	Properties similar to particular sub-function when approaching the corresponding optimum
	30	Composition Function 2	COMPOSITION2	
	31	Composition Function 3	COMPOSITION3	
	32	Composition Function 4	COMPOSITION4	
	33	Composition Function 5	COMPOSITION5	
	34	Composition Function 6	COMPOSITION6	
	35	Composition Function 7	COMPOSITION7	
	36	Composition Function 8	COMPOSITION8	
Search Space: $[-100, 100]^D$, $f_{opt} = 100$				

Table 2. Speedup (single Precision)

D	NO.3	NO.4	NO.5	NO.8	NO.9	NO.10	NO.11	NO.13	NO.14	NO.15
10	0.59	0.20	0.18	12.23	0.49	0.28	0.31	0.32	0.14	0.77
32	3.82	2.42	2.00	47.19	3.54	1.67	3.83	5.09	2.06	3.54
64	4.67	2.72	2.29	50.17	3.56	0.93	3.06	2.88	2.20	3.39
94	13.40	10.10	8.50	84.31	11.13	1.82	9.98	9.66	8.75	6.73
D	NO.16	NO.17	NO.19	NO.20	NO.21	NO.22	NO.23	NO.24	NO.25	NO.26
10	0.80	3.25	0.36	0.20	0.26	0.45	0.63	0.44	2.80	0.52
32	5.57	10.04	3.46	1.22	1.42	6.44	3.95	3.43	11.47	3.36
64	5.45	13.19	3.27	2.10	2.27	3.81	4.62	3.07	14.17	3.34
96	14.38	23.68	11.32	8.26	8.49	11.60	13.67	10.64	30.11	10.71
D	NO.27	NO.28	NO.29	NO.30	NO.31	NO.32	NO.33	NO.34	NO.35	NO.36
10	0.65	0.72	0.70	0.55	0.71	3.49	3.50	0.84	1.28	0.70
32	2.73	3.09	3.63	3.10	4.10	12.39	12.51	5.25	5.19	3.33
64	3.86	4.01	3.21	2.67	3.38	12.68	12.63	3.80	5.27	3.13
96	12.04	11.32	8.15	6.27	8.49	23.67	23.64	9.50	11.79	7.93

Table 3. Speedup (Double Precision)

D	NO.3	NO.4	NO.5	NO.8	NO.9	NO.10	NO.11	NO.13	NO.14	NO.15
10	0.56	0.19	0.17	9.04	0.43	0.26	0.29	0.30	0.14	0.75
32	3.78	2.43	1.80	33.37	3.09	1.59	3.52	4.81	1.97	3.53
64	4.34	2.49	1.93	30.82	3.15	0.92	2.87	2.74	2.11	3.29
96	12.27	9.24	6.95	46.01	9.72	1.78	9.62	8.74	7.87	5.92
D	NO.16	NO.17	NO.19	NO.20	NO.21	NO.22	NO.23	NO.24	NO.25	NO.26
10	0.79	2.32	0.34	0.18	0.26	0.45	0.59	0.43	1.97	0.52
32	5.10	6.79	3.28	1.13	1.29	6.10	3.63	3.14	8.15	3.23
64	4.75	8.29	3.06	1.99	2.18	3.32	4.02	2.77	9.80	2.92
96	11.91	13.81	9.75	7.37	7.78	10.24	11.55	9.57	20.81	9.40
D	NO.27	NO.28	NO.29	NO.30	NO.31	NO.32	NO.33	NO.34	NO.35	NO.36
10	0.79	2.32	0.34	0.18	0.26	0.45	0.59	0.43	1.97	0.52
32	5.10	6.79	3.28	1.13	1.29	6.10	3.63	3.14	8.15	3.23
64	4.75	8.29	3.06	1.99	2.18	3.32	4.02	2.77	9.80	2.92
96	11.91	13.81	9.75	7.37	7.78	10.24	11.55	9.57	20.81	9.40

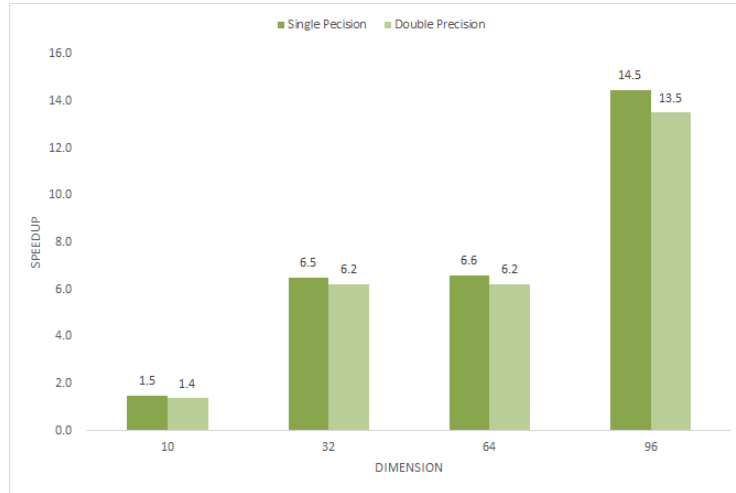


Fig. 1. Overall Speedup

3 Unimodal Functions

3.1 Shifted and Rotated Sphere Function

$$f_1(\mathbf{x}) = \sum_{i=1}^D \mathbf{z}_i^2 + f_{opt} \quad (1)$$

where $\mathbf{z} = \mathbf{R}(\mathbf{x} - \mathbf{x}^{opt})$.

Properties

- Unimodal
- Non-separable
- Highly symmetric, in particular rotationally invariant

3.2 Shifted and Rotated Ellipsoid Function

$$f_4(\mathbf{x}) = \sum_{i=1}^D i \cdot \mathbf{z}_i^2 + f_{opt} \quad (2)$$

where $\mathbf{z} = \mathbf{R}(\mathbf{x} - \mathbf{x}^{opt})$.

Properties

- Unimodal
- Non-separable

3.3 Shifted and Rotated High Conditioned Elliptic Function

$$f_2(\mathbf{x}) = \sum_{i=1}^D (10^6)^{\frac{i-1}{D-1}} \mathbf{z}_i^2 + f_{opt} \quad (3)$$

where $\mathbf{z} = \mathbf{R}(\mathbf{x} - \mathbf{x}^{opt})$.

Properties

- Unimodal
- Non-separable
- Quadratic ill-conditioned
- Smooth local irregularities

3.4 Shifted and Rotated Discus Function

$$f_5(\mathbf{x}) = 10^6 \cdot \mathbf{z}_1^2 + \sum_{i=2}^D \mathbf{z}_i^2 + f_{opt} \quad (4)$$

where $\mathbf{z} = \mathbf{R}(\mathbf{x} - \mathbf{x}^{opt})$.

Properties

- Unimodal
- Non-separable
- Smooth local irregularities
- With One sensitive direction

3.5 Shifted and Rotated Bent Cigar Function

$$f_6(\mathbf{x}) = \mathbf{z}_1^2 + 10^6 \cdot \sum_{i=2}^D \mathbf{z}_i^2 + f_{opt} \quad (5)$$

where $\mathbf{z} = \mathbf{R}(\mathbf{x} - \mathbf{x}^{opt})$.

Properties

- Unimodal
- Non-separable
- Optimum located in a smooth but very narrow valley

3.6 Shifted and Rotated Different Powers Function

$$f_4(\mathbf{x}) = \sqrt{\sum_{i=1}^D |\mathbf{z}_i|^{2+4\frac{i-1}{D-1}}} + f_{opt} \quad (6)$$

where $\mathbf{z} = \mathbf{R}(0.01(\mathbf{x} - \mathbf{x}^{opt}))$.

Properties

- Unimodal
- Non-separable
- Sensitivities of the \mathbf{z}_i -variables are different

3.7 Shifted and Rotated Sharp Valley Function

$$f_4(\mathbf{x}) = \mathbf{z}_i^2 + 100 \cdot \sqrt{\sum_{i=2}^D \mathbf{z}_i^2} + f_{opt} \quad (7)$$

where $\mathbf{z} = \mathbf{R}(\mathbf{x} - \mathbf{x}^{opt})$.

Properties

- Unimodal
- Non-separable
- Global optimum located in a sharp (non-differentiable) ridge

4 Basic Multi-modal Functions

4.1 Shifted and Rotated Step Function

$$f_3(\mathbf{x}) = \sum_{i=1}^D [\mathbf{z}_i + 0.5]^2 + f_{opt} \quad (8)$$

where $\mathbf{z} = \mathbf{R}(\mathbf{x} - \mathbf{x}^{opt})$

Properties

- Many Plateaus of different sizes
- Non-separable

4.2 Shifted and Rotated Weierstrass Function

$$f_9(\mathbf{x}) = \sum_{i=1}^D \left(\sum_{k=0}^{k_{max}} a^k \cos(2\pi b^k (\mathbf{z}_i + 0.5)) \right) - D \cdot \sum_{k=0}^{k_{max}} a^k \cos(2\pi b^k \cdot 0.5) + f_{opt} \quad (9)$$

where $a = 0.5$, $b = 3$, $k_{max} = 20$, $\mathbf{z} = \mathbf{R}(0.005 \cdot (\mathbf{x} - \mathbf{x}^{opt}))$.

Properties

- Multi-modal
- Non-separable
- Continuous everywhere but only differentiable on a set of points

4.3 Shifted and Rotated Griewank Function

$$f_{10}(\mathbf{x}) = \sum_{i=1}^D \frac{\mathbf{z}_i^2}{4000} - \prod_{i=1}^D \cos\left(\frac{\mathbf{z}_i}{\sqrt{i}}\right) + 1 + f_{opt} \quad (10)$$

where $\mathbf{z} = \mathbf{R}(6 \cdot (\mathbf{x} - \mathbf{x}^{opt}))$.

Properties

- Multi-modal
- Non-separable
- With many regularly distributed local optima

4.4 Shifted Rastrigin Function

$$f_{11}(\mathbf{x}) = \sum_{i=1}^D (\mathbf{z}_i^2 - 10 \cos(2\pi\mathbf{z}_i)) + 10 \cdot D + f_{opt} \quad (11)$$

where $\mathbf{z} = 0.0512 \cdot (\mathbf{x} - \mathbf{x}^{opt})$.

Properties

- Multi-modal
- Separable
- With many regularly distributed local optima

4.5 Shifted and Rotated Rastrigin Function

$$f_{12}(\mathbf{x}) = \sum_{i=1}^D (\mathbf{z}_i^2 - 10 \cos(2\pi\mathbf{z}_i) + 10) + f_{opt} \quad (12)$$

where $\mathbf{z} = \mathbf{R}(0.0512 \cdot (\mathbf{x} - \mathbf{x}^{opt}))$.

Properties

- Multi-modal
- Non-separable
- With many regularly distributed local optima

4.6 Shifted Rotated Schaffer's F7 Function

$$f_{17}(\mathbf{x}) = \left(\frac{1}{D-1} \sum_{i=1}^{D-1} ((1 + \sin^2(50 \cdot \mathbf{w}_i^{0.2})) \cdot \sqrt{\mathbf{w}_i}) \right)^2 + f_{opt} \quad (13)$$

where $\mathbf{w}_i = \sqrt{\mathbf{z}_i^2 + \mathbf{z}_{i+1}^2}$, $\mathbf{z} = \mathbf{R}(\mathbf{x} - \mathbf{x}^{opt})$.

Properties

- Multi-modal
- Non-separable

4.7 Expanded Griewank plus Rosenbrock Function

Rosenbrock Function: $g_2(x, y) = 100(x^2 - y)^2 + (x - 1)^2$

Griewank Function: $g_3(x) = x^2/4000 - \cos(x) + 1$

$$f_{18}(\mathbf{x}) = \sum_{i=1}^{D-1} g_3(g_2(\mathbf{z}_i, \mathbf{z}_{i+1})) + g_3(g_2(\mathbf{z}_D, \mathbf{z}_1)) + f_{opt} \quad (14)$$

where $\mathbf{z} = \mathbf{R}(0.05 \cdot (\mathbf{x} - \mathbf{x}^{opt})) + \mathbf{1}$.

Properties

- Multi-modal
- Non-separable
-

4.8 Shifted and Rotated Rosenbrock Function

$$f_7(\mathbf{x}) = \sum_{i=1}^{D-1} (100 \cdot (\mathbf{z}_i^2 - \mathbf{z}_{i+1})^2 + (\mathbf{z}_i - 1)^2) + f_{opt} \quad (15)$$

where $\mathbf{z} = \mathbf{R}(0.02048 \cdot (\mathbf{x} - \mathbf{x}^{opt})) + \mathbf{1}$.

Properties

- Multi-modal
- Non-separable
- With a long, narrow, parabolic shaped flat valley from local optima to global optima

4.9 Shifted Modified Schwefel Function

$$f_{13}(\mathbf{x}) = 418.9829 \times D - \sum_{i=1}^D g_1(\mathbf{w}_i), \quad \mathbf{w}_i = \mathbf{z}_i + 420.9687462275036 \quad (16)$$

$$g_1(\mathbf{w}_i) = \begin{cases} \mathbf{w}_i \cdot \sin(\sqrt{|\mathbf{w}_i|}) & \text{if } |\mathbf{w}_i| \leq 500 \\ (500 - \text{mod}(\mathbf{w}_i, 500)) \cdot \sin\left(\sqrt{500 - \text{mod}(\mathbf{w}_i, 500)}\right) - \frac{(\mathbf{w}_i - 500)^2}{10000D} & \text{if } \mathbf{w}_i > 500 \\ (\text{mod}(-\mathbf{w}_i, 500) - 500) \cdot \sin\left(\sqrt{500 - \text{mod}(-\mathbf{w}_i, 500)}\right) - \frac{(\mathbf{w}_i + 500)^2}{10000D} & \text{if } \mathbf{w}_i < -500 \end{cases} \quad (17)$$

where $\mathbf{z} = 10 \cdot (\mathbf{x} - \mathbf{x}^{opt})$.

Properties

- Multi-modal
- Separable
- Having many local optima with the second better local optima far from the global optima

4.10 Shifted Rotated Modified Schwefel Function

$$f_{14}(\mathbf{x}) = 418.9829 \times D - \sum_{i=1}^D g_1(\mathbf{w}_i), \quad \mathbf{w}_i = \mathbf{z}_i + 420.9687462275036 \quad (18)$$

where $\mathbf{z} = \mathbf{R}(10 \cdot (\mathbf{x} - \mathbf{x}^{opt}))$ and $g_1(\cdot)$ is defined as Eq. 17.

Properties

- Multi-modal
- Non-separable
- Having many local optima with the second better local optima far from the global optima

4.11 Shifted Rotated Katsuura Function

$$f_{15}(\mathbf{x}) = \frac{10}{D^2} \prod_{i=1}^D \left(1 + i \sum_{j=1}^{32} \frac{|2^j \cdot \mathbf{z}_i - [2^j \cdot \mathbf{z}_i]|}{2^j}\right)^{\frac{10}{D^{1.2}}} - \frac{10}{D^2} + f_{opt} \quad (19)$$

where $\mathbf{z} = \mathbf{R}(0.05 \cdot (\mathbf{x} - \mathbf{x}^{opt}))$.

Properties

- Multi-modal
- Non-separable
- Continuous everywhere but differentiable nowhere

4.12 Shifted and Rotated Lunacek bi-Rastrigin Function

$$f_{12}(\mathbf{x}) = \min \left(\sum_{i=1}^D (\mathbf{z}_i - \mu_1)^2, dD + s \sum_{i=1}^D (\mathbf{z}_i - \mu_2)^2 \right) + 10 \cdot \left(D - \sum_{i=1}^D \cos(2\pi(\mathbf{z}_i - \mu_1)) \right) + f_{opt} \quad (20)$$

where $\mathbf{z} = \mathbf{R}(0.1 \cdot (\mathbf{x} - \mathbf{x}^{opt}) + 2.5 * \mathbf{1})$, $\mu_1 = 2.5$, $\mu_2 = -2.5$, $d = 1$, $s = 0.9$.

Properties

- Multi-modal
- Non-separable
- With two funnel around $\mu_1 \mathbf{1}$ and $\mu_2 \mathbf{1}$

4.13 Shifted and Rotated Ackley Function

$$f_8(\mathbf{x}) = -20 \cdot \exp \left(-0.2 \sqrt{\frac{1}{D} \sum_{i=1}^D \mathbf{x}_i^2} \right) - \exp \left(\frac{1}{D} \sum_{i=1}^D \cos(2\pi \mathbf{x}_i) \right) + 20 + e + f_{opt} \quad (21)$$

where $\mathbf{z} = \mathbf{R}(\mathbf{x} - \mathbf{x}^{opt})$.

Properties

- Multi-modal
- Non-separable
- Having many local optima with the global optima located in a very small basin

4.14 Shifted Rotated HappyCat Function

$$f_{16}(\mathbf{x}) = \left| \sum_{i=1}^D \mathbf{z}_i^2 - D \right|^{0.25} + \left(\frac{1}{2} \sum_{j=1}^D \mathbf{z}_j^2 + \sum_{j=1}^D \mathbf{z}_j \right) / D + 0.5 + f_{opt} \quad (22)$$

where $\mathbf{z} = \mathbf{R}(0.05 \cdot (\mathbf{x} - \mathbf{x}^{opt})) - \mathbf{1}$.

Properties

- Multi-modal
- Non-separable
- Global optima located in curved narrow valley

4.15 Shifted Rotated HGBat Function

$$f_{17}(\mathbf{x}) = \left| \left(\sum_{i=1}^D \mathbf{z}_i^2 \right)^2 - \left(\sum_{j=1}^D \mathbf{z}_j^2 \right)^2 \right|^{0.5} + \left(\frac{1}{2} \sum_{j=1}^D \mathbf{z}_j^2 + \sum_{j=1}^D \mathbf{z}_j \right) / D + 0.5 + f_{opt} \quad (23)$$

where $\mathbf{z} = \mathbf{R}(0.05 \cdot (\mathbf{x} - \mathbf{x}^{opt})) - \mathbf{1}$.

Properties

- Multi-modal
- Non-separable
- Global optima located in curved narrow valley

4.16 Expanded Schaffer's F6 Function

$$\text{Schaffer's F6 Function: } g_4(x, y) = \frac{\sin^2(\sqrt{x^2 + y^2}) - 0.5}{(1 + 0.001 \cdot (x^2 + y^2))^2} + 0.5$$

$$f_{19}(\mathbf{x}) = \sum_{i=1}^{D-1} g_4(\mathbf{z}_i, \mathbf{z}_{i+1}) + g_4(\mathbf{z}_D, \mathbf{z}_1) + f_{opt} \quad (24)$$

where $\mathbf{z} = \mathbf{R}(\mathbf{x} - \mathbf{x}^{opt})$.

Properties

- Multi-modal
- Non-separable

5 Hybrid Functions

Hybrid functions are constructed according to [3]. For each hybrid function, the variables are randomly divided into subcomponents and different basic functions (unimodal and multi-modal) are used for different subcomponents, as depicted by Eq. 25.

$$F(\mathbf{x}) = \sum_{i=1}^N G_i(\mathbf{R}_i \cdot \mathbf{z}^i) + f^{opt} \quad (25)$$

where $F(\cdot)$ is the constructed hybrid function and $G_i(\cdot)$ is the i -th basic function used, N is the number of basic functions. \mathbf{z}_i is constructed as follows.

$$\begin{aligned} \mathbf{y} &= \mathbf{x} - \mathbf{x}^{opt} \\ \mathbf{z}^1 &= [\mathbf{y}_{S_1}, \mathbf{y}_{S_2}, \dots, \mathbf{y}_{S_{n_1}}] \\ \mathbf{z}^2 &= [\mathbf{y}_{S_{n_1+1}}, \mathbf{y}_{S_{n_1+2}} \dots \mathbf{y}_{S_{n_1+n_2}}] \\ &\quad \vdots \\ \mathbf{z}^N &= [\mathbf{y}_{S_{(\sum_{i=1}^{N-1} n_i)+1}}, \mathbf{y}_{S_{(\sum_{i=1}^{N-1} n_i)+2}}, \dots, \mathbf{y}_{S_{n_D}}] \end{aligned}$$

where S is a permutation of $(1 : D)$, such that $\mathbf{z} = [\mathbf{z}^1, \mathbf{z}^2, \dots, \mathbf{z}^N]$ forms the transformed vector and $n_i, i = 1, \dots, N$ are the dimensions of the basic functions, which is derived as Eq. 26.

$$n_i = \lceil p_i D \rceil (i = 1, 2, \dots, N-1), n_N = D - \sum_{i=1}^{N-1} n_i \quad (26)$$

p_i is used to control the percentage of each basic functions.

5.1 Hybrid Function 1

- $N = 3$
- $p = [0.3, 0.3, 0.4]$
- G_1 : Modified Schwefel's Function
- G_2 : Rastrigin Function
- G_3 : High Conditioned Elliptic Function

5.2 Hybrid Function 2

- $N = 5$
- $p = [0.3, 0.3, 0.4]$
- G_1 : Bent Cigar Function
- G_2 : HGBat Function
- G_3 : Rastrigin Function

5.3 Hybrid Function 3

- $N = 4$
- $p = [0.2, 0.2, 0.3, 0.3]$
- G_1 : Griewank Function
- G_2 : Weierstrass Function
- G_3 : Rosenbrock Function
- G_4 : Expanded Scaffer's F6 Function

5.4 Hybrid Function 4

- $N = 4$
- $p = [0.2, 0.2, 0.3, 0.3]$
- G_1 : HGBat Function
- G_2 : Discus Function
- G_3 : Expanded Griewank plus Rosenbrock Function
- G_4 : Rastrigin Function

5.5 Hybrid Function 5

- $N = 5$
- $p = [0.1, 0.2, 0.2, 0.2, 0.3]$
- G_1 : Expanded Scaffer's F6 Function
- G_2 : HGBat Function
- G_3 : Rosenbrock Function
- G_4 : Modified Schwefel's Function
- G_5 : High Conditioned Elliptic Function

5.6 Hybrid Function 6

- $N = 5$
- $p = [0.1, 0.2, 0.2, 0.2, 0.3]$
- G_1 : Katsuura Function
- G_2 : HappyCat Function
- G_3 : Expanded Griewank plus Rosenbrock Function
- G_4 : Modified Schwefel's Function
- G_5 : Ackley Function

6 Composition Functions

Composition functions are constructed in the same manner as in [2, 3].

$$F(\mathbf{x}) = \sum_{i=1}^N [\omega_i * (\lambda \cdot G_i(\mathbf{x}) + bias_i)] + f^{opt} \quad (27)$$

- $F(\cdot)$: the constructed composition function
- $G_i(\cdot)$: i -th basic function
- N : number of basic functions used
- $bias_i$: define which optimum is the global optimum
- σ_i : control $G_i(\cdot)$'s coverage range, a small σ_i gives a narrow range for $G_i(\cdot)$
- λ_i : control $G_i(\cdot)$'s height
- ω_i : weighted value for $G_i(\cdot)$, calculated as follows:

$$w_i = \frac{1}{\sqrt{\sum_{j=1}^D (\mathbf{x}_j - \mathbf{x}_j^{opt,i})^2}} \exp\left(-\frac{\sum_{j=1}^D (\mathbf{x}_j - \mathbf{x}_j^{opt,i})^2}{2D\sigma_i^2}\right) \quad (28)$$

where $\mathbf{x}^{opt,i}$ represents the optimum position for $G_i(\cdot)$. Then normalized w_i to get ω_i : $\omega_i = w_i / \sum_{i=1}^N w_i$.

When $\mathbf{x} = \mathbf{x}^{opt,i}$, $\omega_j = \begin{cases} 1 & j = i \\ 0 & j \neq i \end{cases}$ ($j = 1, 2, \dots, N$), such that $F(\mathbf{x}) = bias_i + f^{opt,i}$.

The constructed functions are multi-modal and non-separable and merge the properties of the sub-functions better and maintains continuity around the global/local optima. The local optimum which has the smallest bias value is the global optimum. The optimum of the third basic function is set to the origin as a trip in order to test the algorithms' tendency to converge to the search center.

Note that, the landscape is not only changes along with the selection of basic function, but the optima and σ and λ can effect it greatly.

6.1 Composition Function 1

- $N = 5$
- $\sigma = [10, 20, 30, 40, 50]$
- $\lambda = [1e - 10, 1e - 6, 1e - 26, 1e - 6, 1e - 6]$
- $bias = [0, 100, 200, 300, 400]$
- G_1 : Rotated Rosenbrock Function
- G_2 : High Conditioned Elliptic Function
- G_3 : Rotated Bent Cigar Function
- G_4 : Rotated Discus Function
- G_5 : High Conditioned Elliptic Function

6.2 Composition Function 2

- $N = 3$
- $\sigma = [15, 15, 15]$
- $\lambda = [1, 1, 1]$
- $bias = [0, 100, 200]$
- G_1 : Expanded Schwefel Function
- G_2 : Rotated Rstrigin Function
- G_3 : Rotated HGBat Function

6.3 Composition Function 3

- $N = 3$
- $\sigma = [20, 50, 40]$
- $\lambda = [0.25, 1, 1e - 7]$
- $bias = [0, 100, 200]$
- G_1 : Rotated Schwefel Function
- G_2 : Rotated Rastrigin Function
- G_3 : Rotated High Conditioned Elliptic Function

6.4 Composition Function 4

- $N = 5$
- $\sigma = [20, 15, 10, 10, 40]$
- $\lambda = [2.5e - 2, 0.1, 1e - 8, 0.25, 1]$
- $bias = [0, 100, 200, 300, 400]$
- G_1 : Rotated Schwefel Function
- G_2 : Rotated HappyCat Function
- G_3 : Rotated High Conditioned Elliptic Function
- G_4 : Rotated Weierstrass Function
- G_5 : Rotated Griewank Function

6.5 Composition Function 5

- $N = 5$
- $\sigma = [15, 15, 15, 15, 15]$
- $\lambda = [10, 10, 2.5, 2.5, 1e - 6]$
- $bias = [0, 100, 200, 300, 400]$
- G_1 : Rotated HGBat Function
- G_2 : Rotated Rastrigin Function
- G_5 : Rotated Schwefel Function
- G_4 : Rotated Weierstrass Function
- G_3 : Rotated High Conditioned Elliptic Function

6.6 Composition Function 6

- $N = 5$
- $\sigma = [10, 20, 30, 40, 50]$
- $\lambda = [2.5, 10, 2.5, 5e - 4, 1e - 6]$
- $bias = [0, 100, 200, 300, 400]$
- G_1 : Rotated Expanded Griewank plus Rosenbrock Function
- G_2 : Rotated HappyCat Function
- G_3 : Rotated Schwefel Function
- G_4 : Rotated Expanded Scaffer's F6 Function
- G_5 : High Conditioned Elliptic Function

6.7 Composition Function 7

- $N = 3$
- $\sigma = [10, 30, 50]$
- $\lambda = [1, 1, 1]$
- $bias = [0, 100, 200]$
- G_1 : Hybrid Function 1
- G_2 : Hybrid Function 2
- G_3 : Hybrid Function 3

6.8 Composition Function 8

- $N = 3$
- $\sigma = [10, 30, 50]$
- $\lambda = [1, 1, 1]$
- $bias = [0, 100, 200]$
- G_1 : Hybrid Function 4
- G_2 : Hybrid Function 5
- G_3 : Hybrid Function 6

References

1. Finck, S., Hansen, N., Ros, R., Auger, A.: Real-parameter black-box optimization benchmarking 2010: Noiseless functions definitions. Technical Report 2009/20, Research Center PPE (2010)
2. Liang, J.J., Qu, B.Y., Suganthan, P.N., Hernández-Díaz, A.G.: Problem definitions and evaluation criteria for the cec 2013 special session and competition on real-parameter optimization. Technical Report 201212, Computational Intelligence Laboratory, Zhengzhou University and Nanyang Technological University, Singapore (2013)
3. Liang, J.J., Qu, B.Y., Suganthan, P.N.: Problem definitions and evaluation criteria for the cec 2014 special session and competition on single objective real-parameter numerical optimization. Technical Report 201311, Computational Intelligence Laboratory, Zhengzhou University and Nanyang Technological University, Singapore (2013)

Appendices

A Figures for 2-D Functions

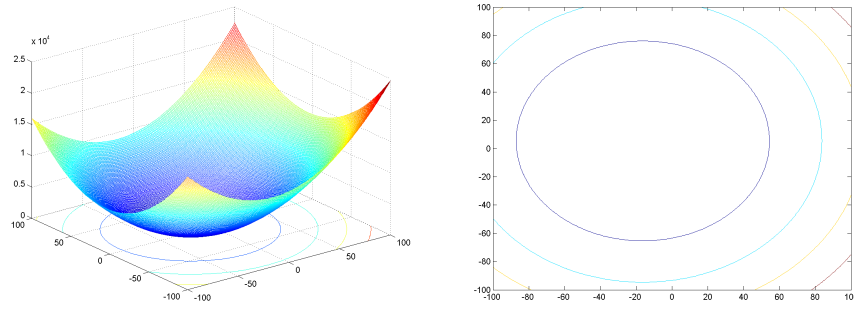


Fig. 2. Sphere Function

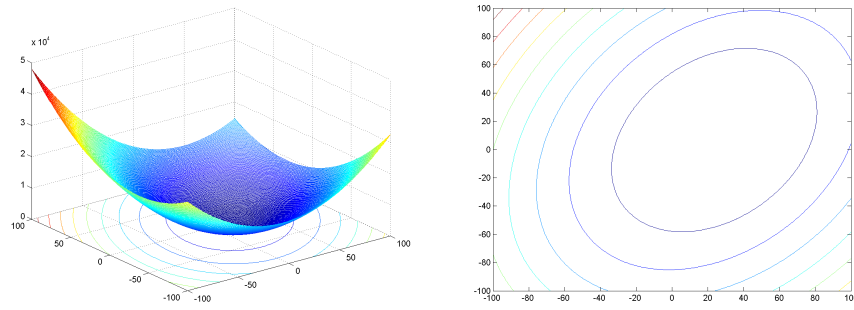


Fig. 3. Ellipsoid Function

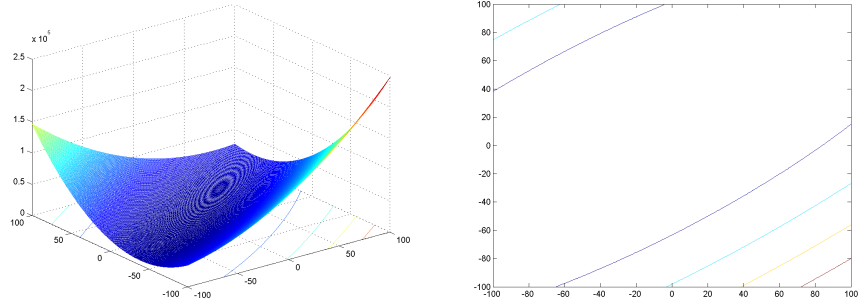


Fig. 4. Elliptic Function

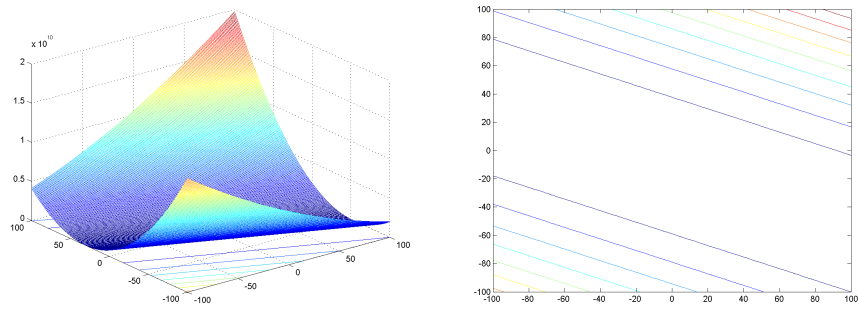


Fig. 5. Discus Function

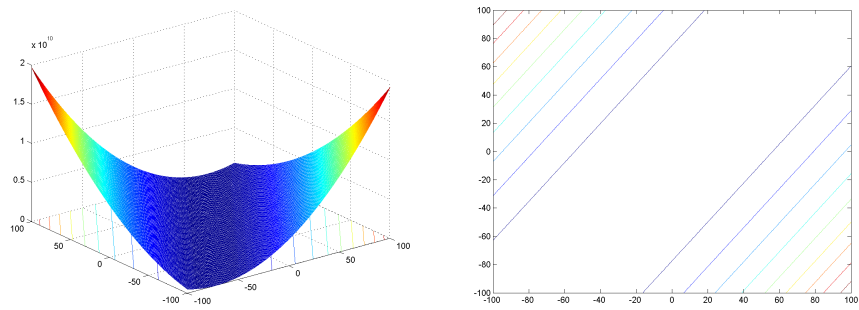


Fig. 6. Bent Cigar Function

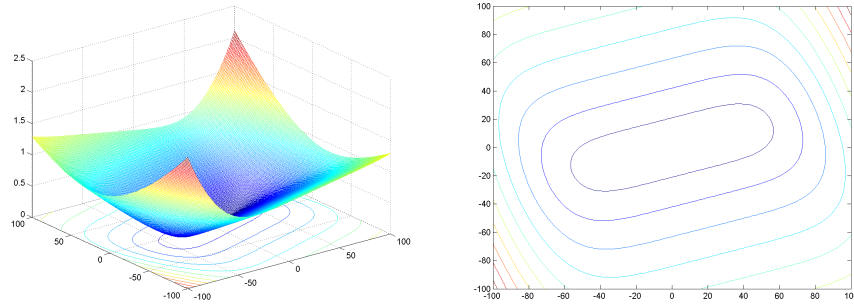


Fig. 7. Different Powers Function

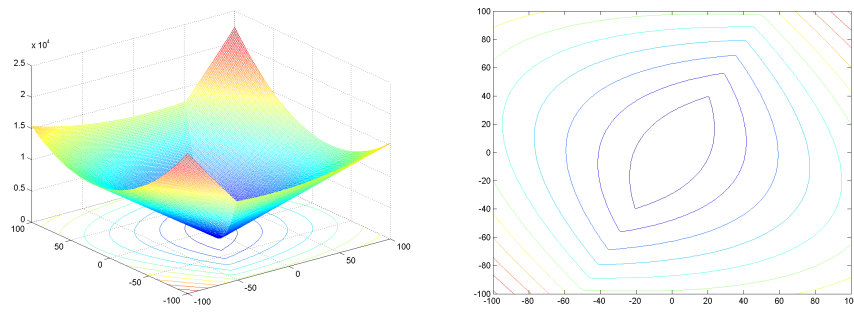


Fig. 8. Sharp Valley Function

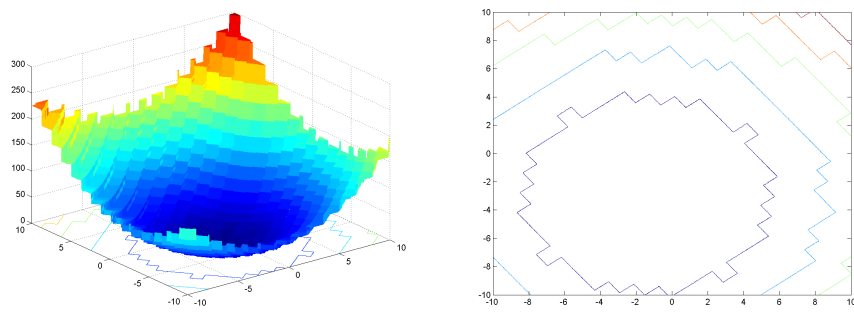


Fig. 9. Step Function

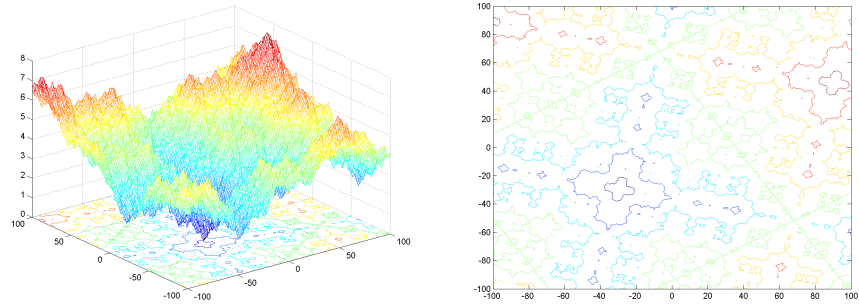


Fig. 10. Weierstrass Function

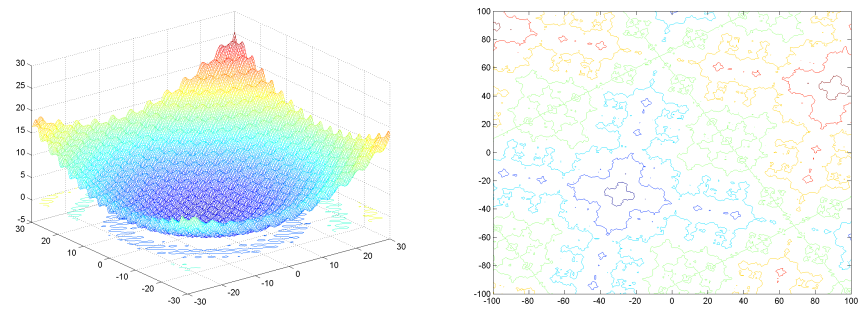


Fig. 11. Weierstrass Function

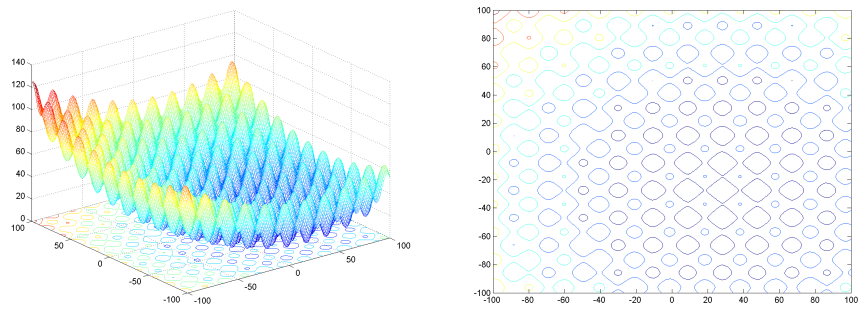


Fig. 12. Rastrigin Function

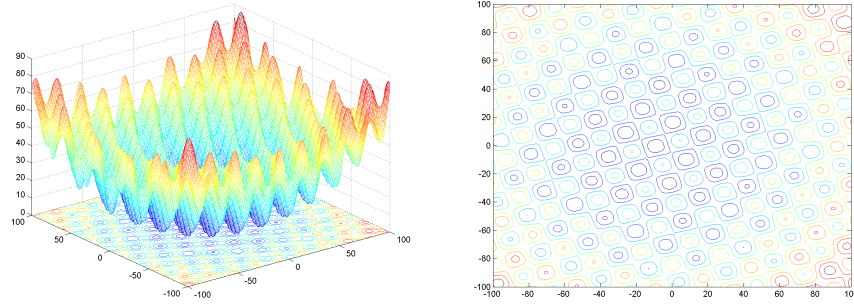


Fig. 13. Rotated Rastrigin Function

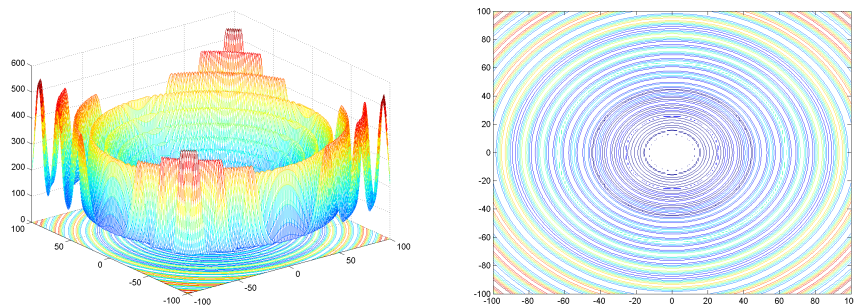


Fig. 14. Schaffer's F7 Function

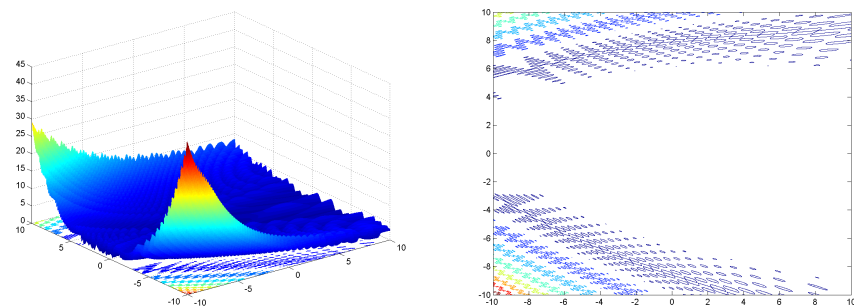


Fig. 15. Expanded Griewank Rosenbrock Function

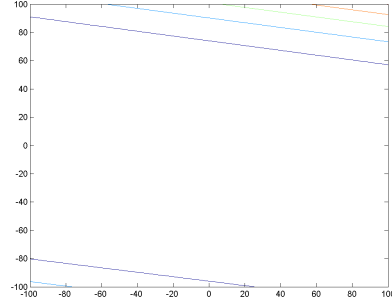
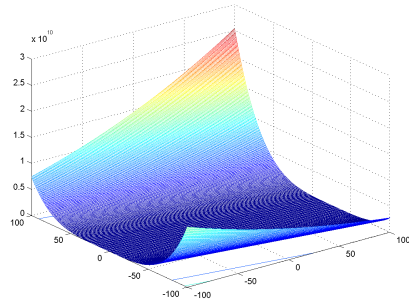


Fig. 16. Rosenbrock Function

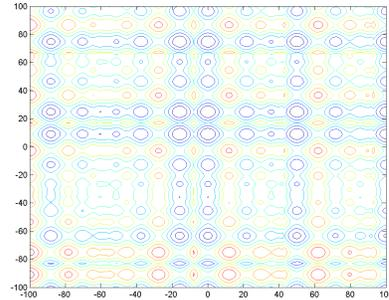
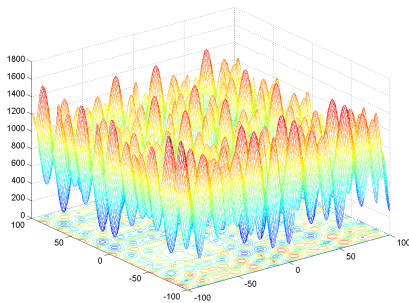


Fig. 17. Schwefel Function

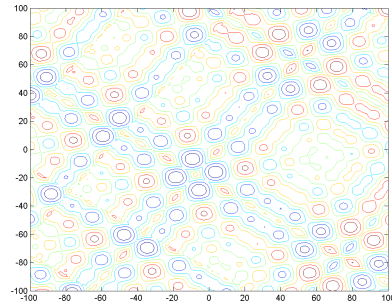
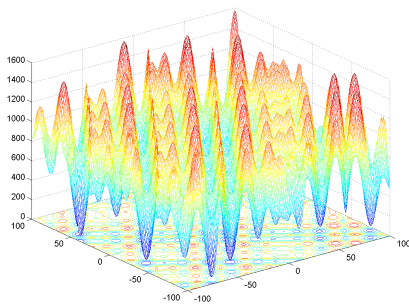


Fig. 18. Rotated Schwefel Function

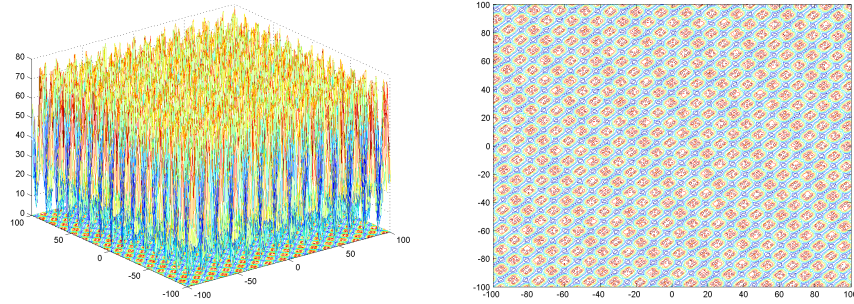


Fig. 19. Katsuura Function

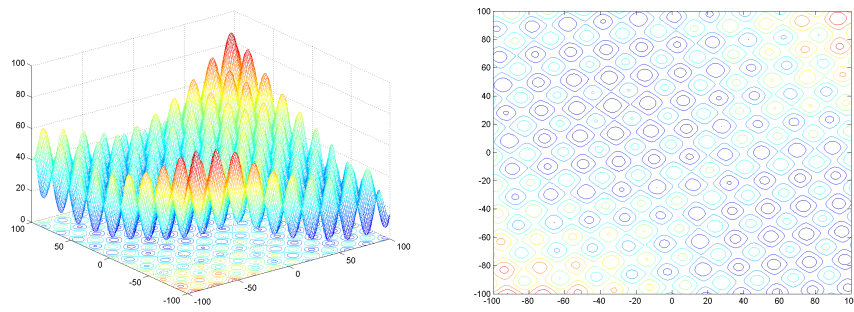


Fig. 20. Lunacek Function

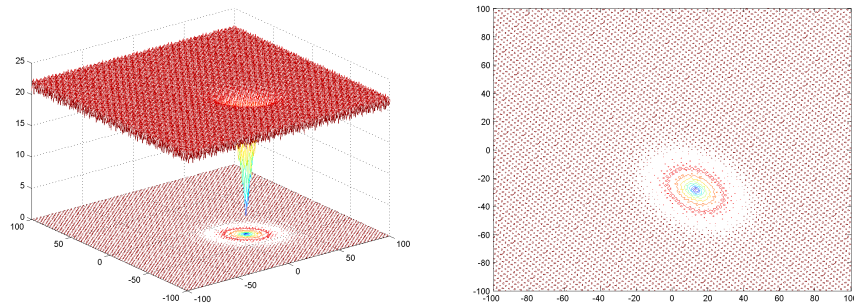


Fig. 21. Ackley Function

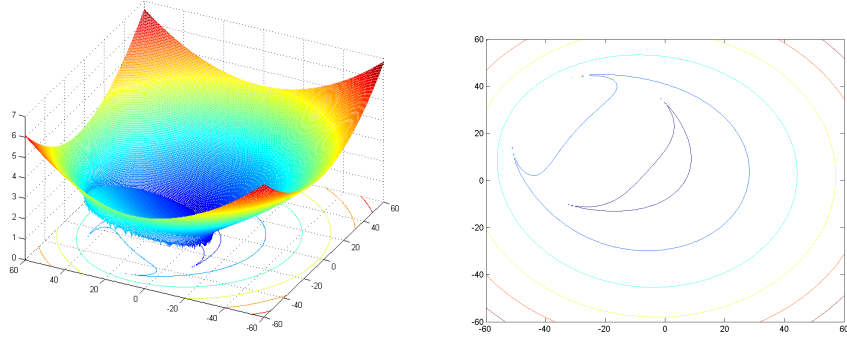


Fig. 22. HappyCat Function

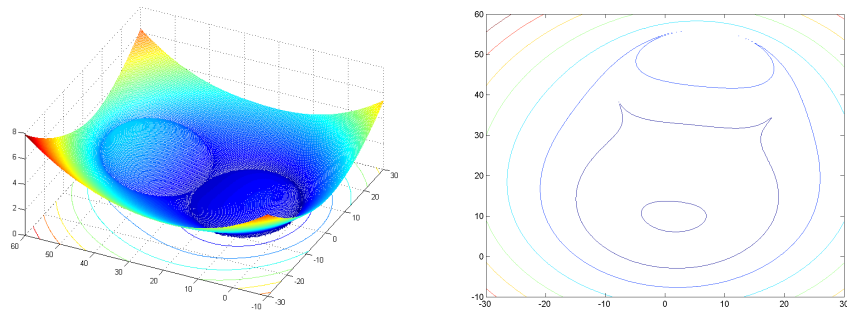


Fig. 23. HGBat Function

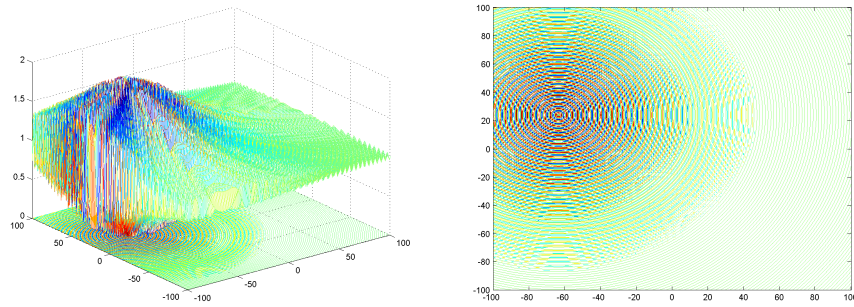


Fig. 24. Expanded Scaffers' F6 Function

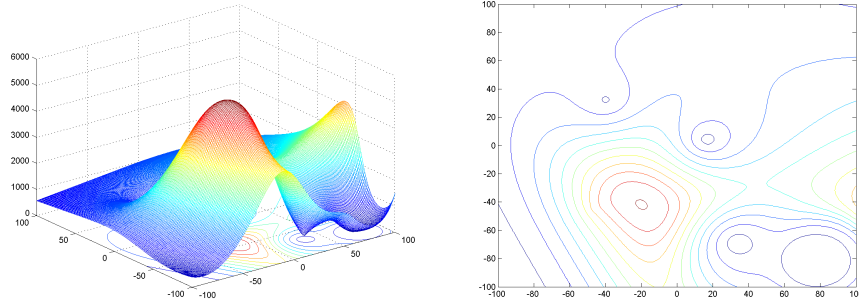


Fig. 25. Composition Function 1

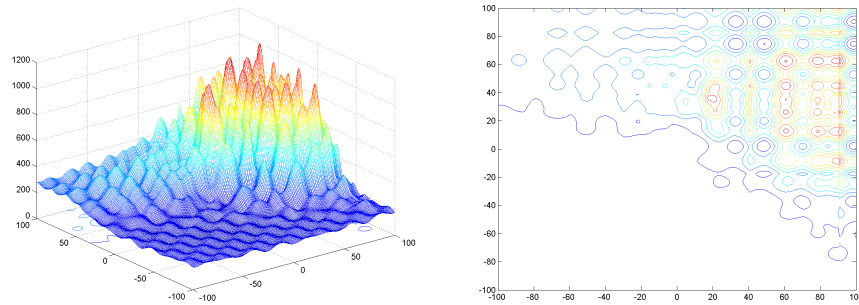


Fig. 26. Composition Function 2

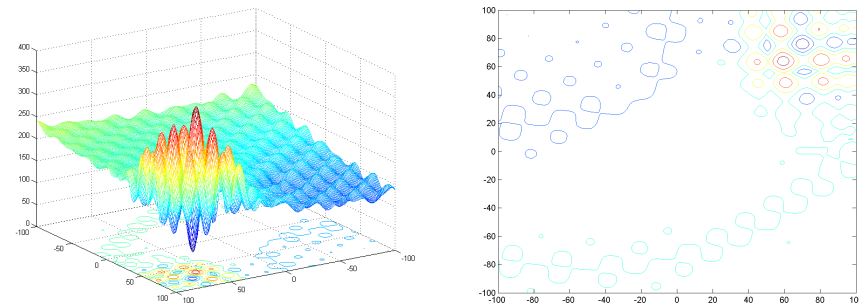


Fig. 27. Composition Function 3

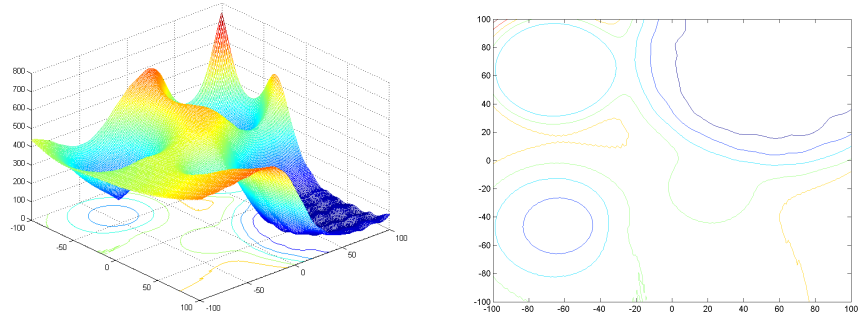


Fig. 28. Composition Function 4

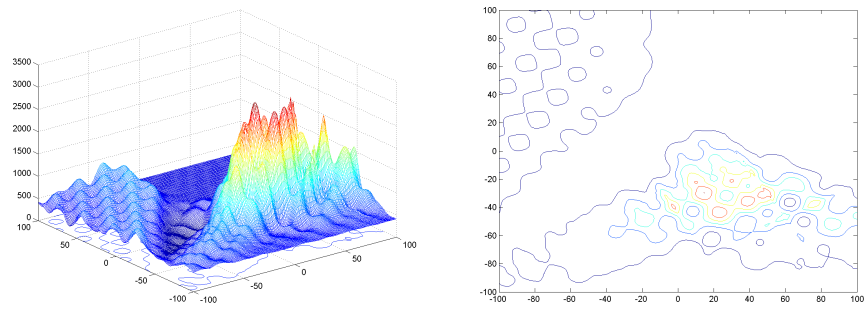


Fig. 29. Composition Function 5

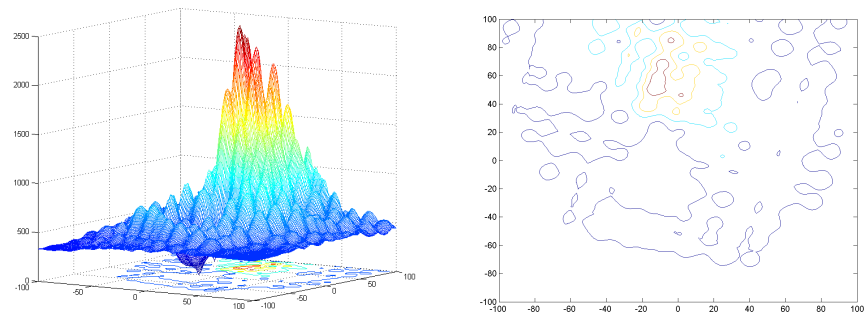


Fig. 30. Composition Function 6